Journal of the European Ceramic Society 21 (2001) 2301–2309

www.elsevier.com/locate/jeurceramsoc

Processing, microstructure and properties of $LaCoO_{3-\delta}$ ceramics

V.V. Kharton [a,b,*], F.M. Figueiredo [b,c], A.V. Kovalevsky [a], A.P. Viskup [a], E.N. Naumovich [a], A.A. Yaremchenko [a], I.A. Bashmakov [a], F.M.B. Marques [b]

[a] *Institute of Physicochemical Problems, Belarus State University, 14 Leningradskaya Str., 220080 Minsk, Republic of Belarus*
[b] *Department of Ceramics and Glass Engineering, UIMC, University of Aveiro, 3810-193 Aveiro, Portugal*
[c] *Science and Technology Department, Universidade Aberta, R. Esc. Politecnica 147, 1269-001 Lisbon, Portugal*

Received 16 November 2000; received in revised form 27 December 2000; accepted 12 January 2001

Abstract

Dense lanthanum cobaltite ceramics with different microstructures were prepared using several processing procedures, including chemical and ceramic synthesis routes. XRD, SEM, dilatometry, total electrical conductivity and oxygen permeability measurements were used for the characterization of these materials. Submicrometer size $LaCoO_{3-\delta}$ powders obtained via a cellulose-precursor technique or a combustion synthesis process showed much higher sinterability and poor compactability with respect to the powder prepared by the standard ceramic procedure. The influence of the processing route on crystal lattice, electronic conductivity and thermal expansion of $LaCoO_{3-\delta}$ ceramics was negligible. At the same time, the preparation technique significantly affects the ceramic microstructure and the oxygen ionic conductivity. $LaCoO_{3-\delta}$ membranes prepared via the standard ceramic technique, involving higher sintering temperatures, exhibit significantly higher oxygen permeation fluxes than ceramics prepared from organic precursors. This behavior was attributed to the effect of grain-boundary resistivity to ionic transport, which decreases with increasing sintering temperature and grain size, as commonly found for oxide solid electrolytes.

Keywords: Electrical conductivity; Ionic conductivity; $LaCoO_3$; Perovskites; Thermal expansion

1. Introduction

Solid solutions based on perovskite-type lanthanum cobaltite, $LaCoO_{3-\delta}$, are of interest for numerous applications, including solid oxide fuel cells (SOFCs), oxygen separation membranes, catalysts, lasers and sensors.[1–7] This is due to excellent transport and electrocatalytical properties of cobaltites: high electronic conductivity, significant oxygen ion mobility, and noticeable electrochemical and catalytic activity in reactions involving oxygen. Appropriate A- and B-site doping of the ABO_3 perovskite makes it possible to optimize these properties to a considerable extent.

Lanthanum cobaltite has a rhombohedrally distorted perovskite structure and moderate oxygen deficiency at elevated temperatures, which increases with reducing oxygen partial pressure almost proportional to $p(O_2)^{-1/2}$.[8–10] The electronic conduction in $LaCoO_{3-\delta}$ occurs by transfer of charge carriers via Co–O–Co bonds and exceeds ionic conductivity more than 1000 times.[10–13] In the temperature range 110 K $< T <$ 350 K, excitation of electrons from a narrow valence band to localized states at high-spin cobalt sites introduces mobile small-polaron holes and trapped electrons at stationary Co^{2+} ions.[10] Increasing temperature above 650 K leads to stabilization of a metallic phase containing high-spin Co^{3+} and intermediate-spin Co(III), with the partially filled σ^*_α band responsible for the p-type conductivity.[10] Diffusion of oxygen ions in $LaCoO_{3-\delta}$ occurs via a vacancy mechanism.[14,15]

The present work continues our study of $LaCoO_{3-\delta}$-based materials, with particular emphasis on ionic transport properties.[12,16–21] It has been recently found [21] that processing conditions may significantly affect the oxygen ionic conductivity of lanthanum cobaltite ceramics, probably due to an extremely important role of

* Corresponding author at present address: Department of Ceramics and Glass Engineering, UIMC, University of Aveiro, 3810-193 Aveiro, Portugal. Tel.: +351-234-370263; fax: +351-234-425300.
E-mail address: kharton@cv.ua.pt (V.V. Kharton).

0955-2219/01/$ - see front matter
PII: S0955-2219(01)00199-6

grain boundaries. The oxygen diffusion through dense ceramic membranes of $LaCoO_{3-\delta}$ was ascertained to increase with increasing sintering temperature and grain size.[21] Such behavior is quite typical for oxide solid electrolyte materials, where increasing grain size larger than 1–5 μm leads, as a rule, to reducing the contribution of grain boundary resistivity to the total electrolyte resistance, caused by decreasing grain boundary area.[22–25] In the case of ceramics with a predominant electronic conduction, however, revealing grain-boundary effects on ionic transport is complicated due to numerous experimental constraints, associated with determination of minor contributions to the total conductivity. In fact, literature contains scarce data on this subject, often in contradiction.[26,27]

The optimization of mixed-conducting ceramics for electrochemical applications requires an exact knowledge of relationships between processing conditions, microstructure and physicochemical properties. The evaluation of the effect of different processing routes on the properties of $LaCoO_{3-\delta}$ powders and ceramics, including compactability, sinterability, thermal expansion, electronic conductivity and oxygen permeability is the objective of the present work.

2. Experimental

Two major methods were used to prepare $LaCoO_{3-\delta}$ powders. The first of them, a standard ceramic synthesis technique, is hereafter referred to as Method 1. Mixtures of high-purity $La(NO_3)_3{\cdot}6H_2O$ and $Co(NO_3)_2{\cdot}6H_2O$ taken in stoichiometric proportions were dissolved in a solution of nitric acid, dried and then thermally decomposed. The solid-state reaction was conducted in air at temperatures of 1470–1520 K for 15–20 h, with multiple intermediate grinding steps. Gas-tight ceramic specimens were pressed (280–350 MPa) in the shape of bars ($4\times4\times30$ mm^3) and disks of various thickness (diameter 12 or 15 mm), and then sintered in air at 1750–1770 K for 5–15 h.

In the second preparation route, Method 2, one cellulose precursor was used as described elsewhere.[27–29] Briefly, this method is based on a structure-modified cellulose containing the metal salts as a precursor for the oxide phase synthesis. The starting cellulose fibre is reacted with a 68–70% solution of nitric acid.[28] The interaction of HNO_3 monohydrate with native cellulose results in formation of the so-called Knecht compound-KC, $(C_6H_{10}O_5{\cdot}HNO_3)_n$. KC is then converted into cellulose hydrate (cellulose-II) by the action of water. The phase transformation "cellulose-I→KC→cellulose-II" increases the sorption activity of the cellulose matrix.[28] Incorporation of cations into the modified cellulose was performed by impregnation with a solution containing lanthanum and cobalt nitrates with a cation concentration ratio of 1:1. The impregnation ratio was 1.2 ml/g.[27,28] Then the cellulose fiber is dried in air and ignited, and the $LaCoO_{3-\delta}$ oxide phase is formed in the combustion front. The oxide obtained in this manner retains the fibre precursor texture (Fig. 1A and B) and can be easily converted into a powder with submicron particle size by light mechanical action.

Lastly, a commercial $LaCoO_{3-\delta}$ powder (Praxair Specialty Ceramics, Seattle, USA), having a submicron particle size (Fig. 2A), and prepared by combustion synthesis, was also used for the preparation of ceramic membranes.

All ceramic materials studied in this work and corresponding abbreviations are listed in Table 1. LC-0 corresponds to $LaCoO_{3-\delta}$ ceramics prepared by the standard ceramic technique. LC-100 is used for ceramics obtained by the cellulose-precursor technique. LC-50 samples were prepared from a mixture (50:50 wt.%) of powders synthesized by Methods 1 and 2. Sintering of LC-50 and LC-100 ceramics was performed in air at 1640–1680 K for 7–12 h. Ceramics prepared from the commercial powder, identified as LC-S, were pressed and sintered in air at 1670 K for 2 h.

In order to obtain an oxygen content as close as possible to equilibrium in air at low temperature, dense ceramics were annealed for 5–6 h in air at 1270–1320 K and then cooled down to room temperature with a rate of about 2 K/min prior to further study. After this treatment, nonstoichiometry approached a steady condition, presumably close to equilibrium. No considerable changes in the X-ray diffraction (XRD) patterns were found for samples kept in air at ambient temperature for 100–150 days. Also, no effects indicating a metastable oxygen content in the ceramics were detected by differential thermal and thermal gravimetric analysis (DTA/TGA) on heating.

The experimental procedure and equipment for XRD, DTA/TGA, cation analysis, scanning electron microscopy (SEM), mechanical tests, dilatometry, testing gas tightness, measurements of oxygen permeability and electrical conductivity (4-probe DC) were described in detail elsewhere.[12,16–21,27–29] According to the XRD results, all materials were single phase and the scatter in unit cell parameters of ceramics prepared by the different methods was within the limits of experimental uncertainty. The ratio between experimental and theoretical density (ρ_{exp}/ρ_{theor}) was in the range 91–92% for LC-0, LC-50 and LC-100. For LC-S this ratio was about 97%, with the theoretical density calculated assuming zero oxygen non-stoichiometry ($\delta = 0$). Only samples which had been previously verified to be gas tight, were used for the permeation measurements. Emission spectroscopic analysis used to verify the cation composition of powders and ceramics, showed that the total impurity content in the specimens was less than 0.05 at.%.

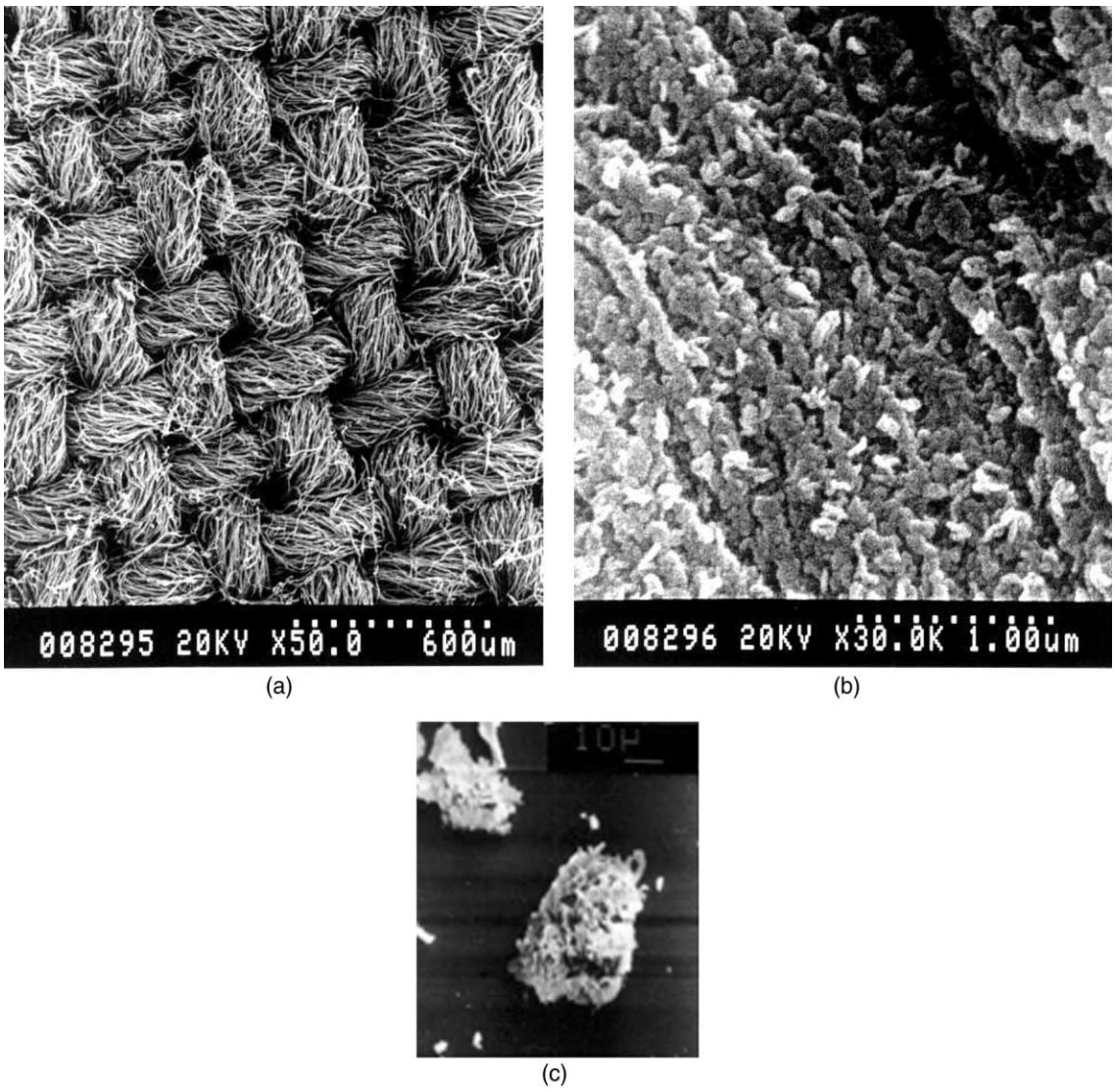

Fig. 1. SEM micrographs of $LaCoO_{3-\delta}$ oxide fibers prepared by Method 2: A and B — fibers after combustion of the cellulose matrix, C — particle agglomerate after mechanical decomposition of the fibers.

Table 1
Abbreviations and processing conditions of $LaCoO_{3-\delta}$ ceramics

Abbreviation	Powder preparation	Sintering temperature (K)	Grain size range (μm)
LC-O	Standard ceramic technique (Method 1)	1750–1770	40–100
LC-100	Cellulose precursor technique (Method 2)	1640–1660	0.5–5
LC-50	Mixture of powders prepared by Methods 1 and 2 (50:50 wt.%)	1650–1680	10–80
LC-S	Praxair specialty chemicals (combustion synthesis)	1670	0.5–5

3. Results and discussion

3.1. Compactability and sinterability

Pressing and sintering of $LaCoO_{3-\delta}$ ceramics demonstrated that the submicron-size powders prepared either by cellulose precursor technique or the combustion technology exhibit poor compactability but superior sinterability when compared to the powder prepared by the standard ceramic technique. Fig. 3 presents data on the pressure dependence of the green density of pressed lanthanum cobaltite powders. At pressures below 250 MPa, the density of LC-100 green compacts was less than 65% of the theoretical density calculated from the XRD results. A similar value was found for LC-S, whereas the density of LC-0 compacts almost reached

80% of the theoretical density. Probable reasons for this behavior refer to agglomeration of particles in the submicron powders, and to a significantly wider range of particle-size in the case of the standard ceramic technique, providing closer packing. Also, intragrain porosity of the powder prepared by Method 2, and mechanical decomposition of large particles obtained using Method 1 could influence the compactability. As an example, Fig. 1C presents SEM image of one agglomerate formed in the powder prepared by the cellulose-precursor method. Some agglomeration was observed also in the LC-S powder (Fig. 2B).

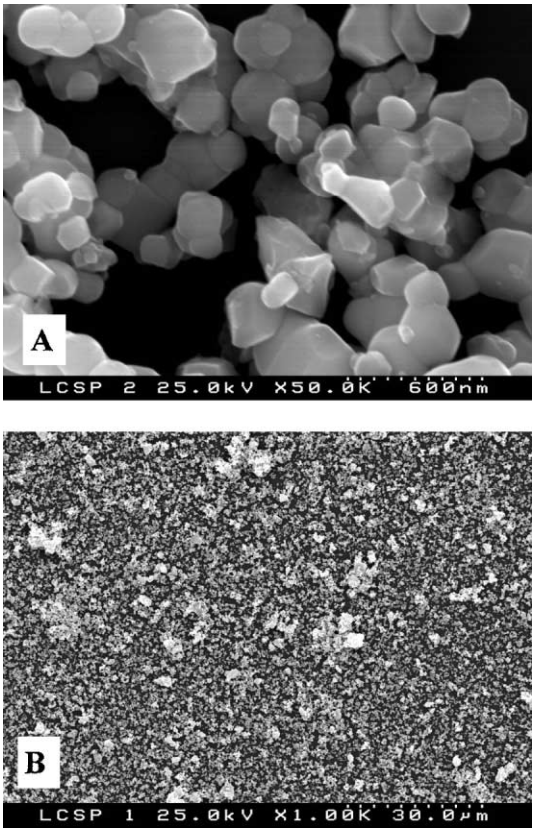

Fig. 2. SEM micrographs of the $LaCoO_{3-\delta}$ powder (PSC) used for the preparation of the LC-S series of ceramics.

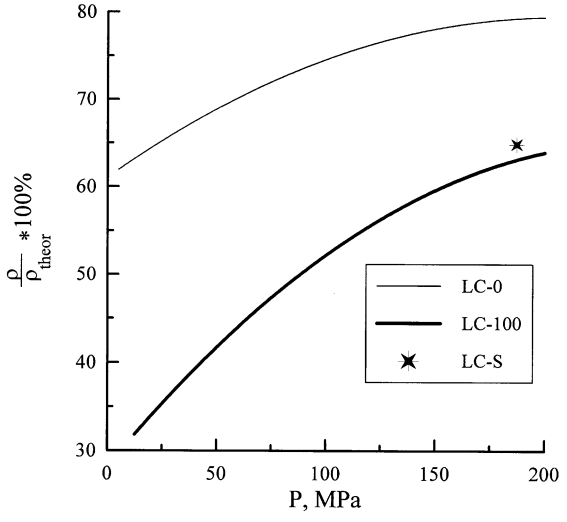

Fig. 3. Dependence of the relative density of $LaCoO_{3-\delta}$ green compacts of lanthanum cobaltite (expressed as % of theoretical density), on the uniaxial pressure.

As opposed to the observed poor compactability, the sinterability of the submicrometer sized powders with high reactivity is 2–3 times greater than that of LC-0 green compacts. Table 2 lists the values of shrinkage after sintering at 1670 K. Again, the shrinkage of LC-100 is close to LC-S, suggesting similar activity of the powders prepared by the cellulose-precursor and combustion methods. The sintering temperature of gas-tight ceramics could be reduced by about 100 K using these powders (Table 1).

The results on compactability and sinterability of LC-100 and LC-S are similar to data already reported in the literature obtained with a fine-grained $LaCoO_{3-\delta}$ powder prepared by the EDTA method.[13]. The density of green compacts, isostatically pressed at 400 MPa,[13] was only 54% of the theoretical density. Further sintering of these green compacts at 1420 K resulted in a relative density of ceramics as high as about 98%.[13] It should also be mentioned that increasing shrinkage with decreasing particle size, commonly found in the case of oxides,[30] may introduce problems in the fabrication of large ceramics from highly reactive powders prepared using organic precursors.

3.2. Microstructure

Designing of different microstructures can usually be obtained by changing the sintering time and temperature for a given processing route and type of precursors. As an alternative, different processing routes (e.g. chemical and ceramic, as used in this work) should also provide ceramics with different microstructures, even using the same sintering conditions. As previously mentioned, a combination of both approaches was adopted in the present case. Furthermore, the need for dense ceramics to be used in the permeation experiments, without open porosity,

Table 2
Shrinkage of $LaCoO_{3-\delta}$ membrane disks pressed at 230 MPa and sintered at 1670±10 K

Abbreviation	Sintering time (h)	Shrinkage in diameter ($\Delta D/D_0$ (%))	Shrinkage in thickness ($\Delta T/T_0$ (%))
LC-0	4	10	6
	7	10	6
LC-100	4	27	14
	7	28	14
LC-S	2	26	15
	4	27	15

established to a reasonable extent the sintering conditions required for each kind of precursor used in this work. This means that the adopted processing routes were not selected for being the most appropriate for the production of these ceramics but rather for providing important microstructural differences. This was a basic requirement for the understanding of the role of microstructural features on the transport of oxygen (a minority charge carrier) through these ceramics.

Fig. 4 illustrates the characteristic microstructures of sintered $LaCoO_{3-\delta}$ ceramics observed by SEM. The smallest grain size, varying from 0.1 to 5 μm, was obtained in the cases of LC-100 and LC-S. Sintering of the starting submicron particles resulted in the formation of larger agglomerates of up to 3–4 μm for LC-S or 20 μm in the case of LC-100. The grain size for LC-50 was considerably larger (up to 80 μm); grain growth and sintering were favored by the presence of the dispersed reactive powder prepared by Method 2. Closed pores in this case, similar to LC-0 and LC-S, were mainly formed by close-packed oxide grains.

The LC-0 ceramics consisted of large grains (40–100 μm) covered by relatively small particles (effective diameter of up to 5 μm). Taking into account that $LaCoO_{3-\delta}$ is characterized by incongruent melting at temperatures close to the sintering temperature of LC-0,[6] sintering of LC-0 is likely to occur via a liquid phase assisted process.[30] The magnified section of Fig. 4A (right) indeed suggests the formation of a liquid phase along the grain boundaries. As a result, the local composition of grain boundaries in LC-0 may differ from the bulk.

Due to the high reactivity of the powders obtained by the cellulose-precursor and combustion methods, the sintering temperature necessary to obtain gas-tight ceramics of LC-100, LC-50 and LC-S series is significantly lower (Table 1). Thus, the sintering mechanism in these cases should be different from that suggested for LC-0. This shows that LC-0 is a specific case within the set of compositions prepared in this work, corresponding to unique sintering conditions and a singular microstructure. This fact is of major importance for the ulterior discussion on oxygen permeation.

3.3. Thermal expansion and electrical conductivity

Irrespective of previously reported differences in microstructure, all materials exhibit similar thermal expansion (Fig. 5). In the temperature range 300–1100 K, dilatometric curves of $LaCoO_{3-\delta}$ ceramics can be approximated by straight lines. The average thermal expansion coefficients (TECs) are close to each other

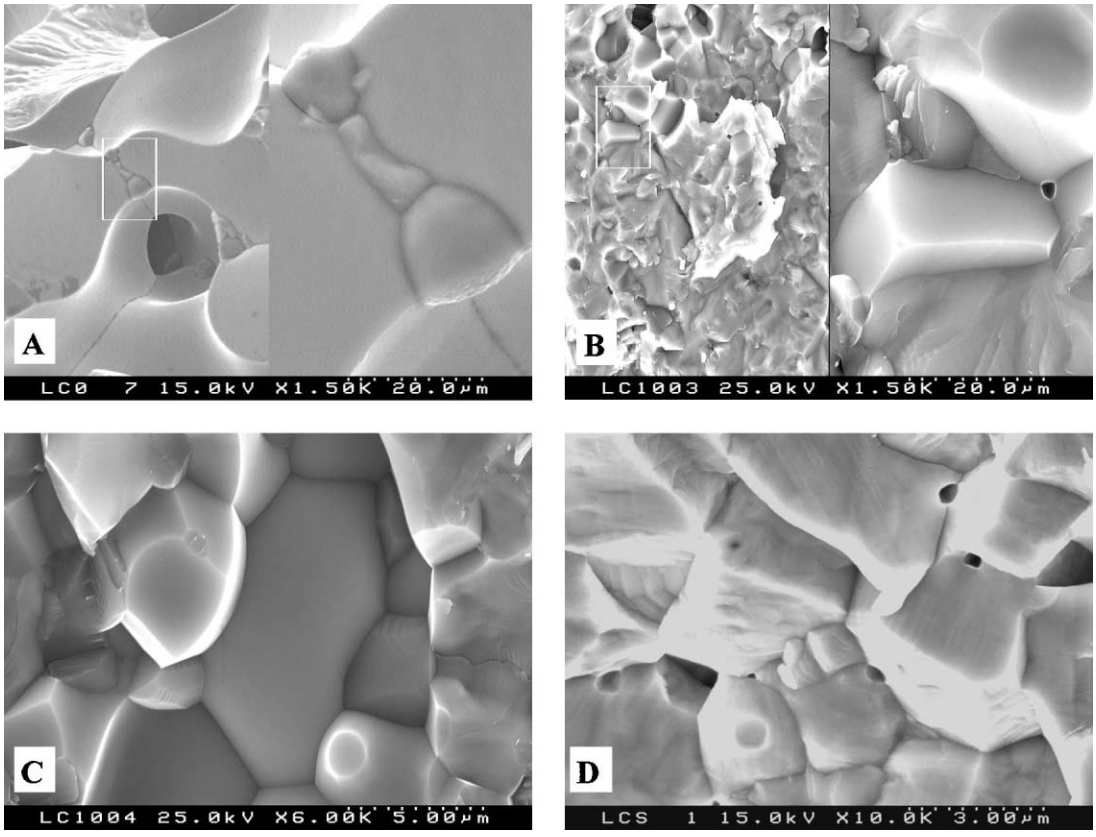

Fig. 4. SEM micrographs of the $LaCoO_{3-\delta}$ ceramics: LC-0 (A), LC-100 (B and C), LC-S (D). The scale and magnification of the micrographs A and B correspond to their left sections. The right sections represent the area within the frame, magnified five times.

within the limits of experimental error (in the order of 21.10^{-6} K^{-1}). This fact is not surprising as thermal expansion is determined by the volume fraction and type of connectivity of phases present in the ceramics. In these cases the ceramics are typically phase-pure and the grain size is large when compared to the characteristic dimensions of minor secondary phases, either amorphous or crystalline, which may form along the grain boundaries. The chemical expansion caused by the oxygen losses in the course of heating should also be similar for all materials under study.

As for thermal expansion, the total conductivity of $LaCoO_{3-\delta}$ (predominantly electronic) is independent of the preparation technique and microstructural differences, within the limits of experimental error (Table 3). This indicates negligible effect of grain boundaries on the electronic transport, a common observation for oxides with high electronic conductivity when the porosity is less than 10%.[6,31] In this case, the main factors determining the conductivity are the cation composition and oxygen content.[6,31] Since all materials have similar grain bulk composition (both A/B- cation ratio, and (A + B)/O - metal to oxygen ratio) and low porosity, the differences in electronic conductivity are negligible.

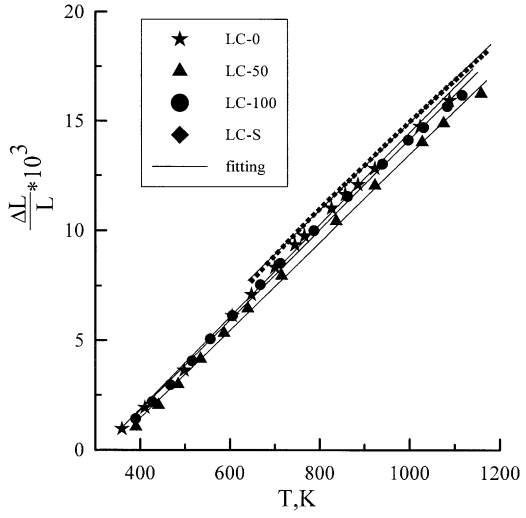

Fig. 5. Temperature dependence of relative elongation of $LaCoO_{3-\delta}$ ceramics in air. Solid lines correspond to the linear model for thermal expansion.

Table 3
Total electrical conductivity of $LaCoO_{3-\delta}$ ceramics in air

Material	σ (S/cm)		
	1223 K	1073 K	773 K
LC-0	9.1×10^2	9.4×10^2	8.4×10^2
LC-50	8.8×10^2	9.1×10^2	7.5×10^2
LC-100	8.8×10^2	9.0×10^2	7.3×10^2
LC-S	8.7×10^2	9.4×10^2	7.6×10^2

3.4. Oxygen permeability

For a cell under a given oxygen activity gradient, the effective permeation flux density j (expressed in $mol\times s^{-1}\times cm^{-2}$) through the cell and the specific oxygen permeability $J(O_2)$ (expressed in $mol\times s^{-1}\times cm^{-1}$) can be related by:

$$J(O_2) = j\cdot d\cdot\left[\ln\frac{p_2}{p_1}\right]^{-1} \quad (1)$$

These are the most relevant parameters which can be used to discuss oxygen permeation data. In this equation d is the thickness of the sample, and p_2 and p_1 the oxygen partial pressures at the membrane feed and permeate sides, respectively. For materials obeying the Wagner's law, with the permeability exclusively governed by the ionic and electronic transport properties, the specific oxygen permeability should be constant, irrespective of the cell thickness.

Selected results on oxygen permeation through $LaCoO_{3-\delta}$ membranes are given in Fig. 6. In contrast with other ceramic materials, LC-0 membranes exhibit

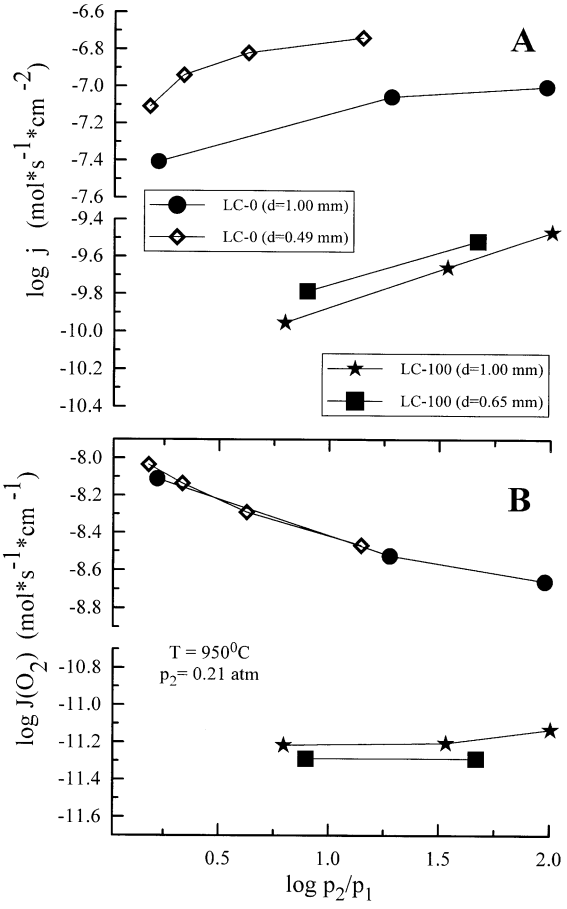

Fig. 6. Dependence of oxygen permeation flux density (A) and specific oxygen permeability (B) of lanthanum cobaltite ceramics on oxygen partial pressure gradient.

extremely long stabilization processes under an oxygen chemical potential gradient, as illustrated in Fig. 7. Up to 700 h are needed to reach a steady-state condition. Analogous behavior was reported earlier for $La(Co,Cr)O_{3-\delta}$ ceramics.[32] The negligible dependencies of the permeation fluxes on LC-0 membrane thickness (Fig. 6B) show no surface exchange limitations during the transient period. Hence, the explanation introduced by ten Elshof et al.,[33] who attributed to a surface effect a similar behavior observed with $La(Sr)FeO_{3-\delta}$ solid solutions, may not be applied in the present case.

Besides surface effects, structural changes could also explain this long transient behavior of LC-0. However, no such changes were identified by XRD tests performed after the permeation experiments with LC-0 membranes. As a last possibility, the observed behavior might be ascribed to the role of minor percentages of glassy phases found along grain boundaries, either due to crystallization or to some exudation which might occur from loss of solubility of minor impurities at low temperature. In general, both processes would be coherent with the higher sintering temperature used while processing LC-0 samples, and with the traces of liquid phase formation observed by SEM (Fig. 4A).

Overall, the oxygen permeability within the exploited temperature range increases in the sequence LC-100 < LC-50 ⩽ LC-S < LC-0 (Fig. 8). When comparing the membranes prepared by the standard ceramic and cellulose-precursor techniques, this behavior may be attributed to increasing average grain size, in the order LC-100 < LC-50 < LC-0, and lower grain-boundary resistance to ionic transport. In the case of solid oxide electrolytes, an increase in sintering temperature leads, as a rule, to a lower grain-boundary resistivity.[22,25] A parallel explanation can be used in the present case. In fact, LC-0 membranes with maximum permeability were sintered at higher temperatures with respect to the remaining lanthanum cobaltite ceramics (Table 1).

One should note that the relatively low oxygen permeability of LC-100 ceramics may partially result from with non-negligible surface limitations. In this case, increasing membrane thickness leads to higher $J(O_2)$ values, caused by a decreasing role of the oxygen surface exchange on the permeation flux (Fig. 6). Therefore, oxygen interphase exchange rate decreases with decreasing grain size, similar to the ionic conductivity. Such an influence is associated, firstly, with well-known correlation between surface exchange and bulk oxygen diffusion. Also, changes in the processing route may affect surface microstructure, including surface concentration of active adsorption centers.

The only ceramics not following the simple correlation between oxygen permeability and grain size are those identified as LC-S. In fact in this case we have ceramics with relatively small grain size, high grain boundary density and reasonably high permeability. This can only be explained by a different nature of grain boundaries, determined by a specific synthesis route and level and type of impurities. The LC-S ceramics were based on a commercial powder, and the processing steps can be considered unique with respect to all other samples. Grain boundaries are in fact a complex entity and simple correlation between grain size and grain boundary performance is only possible when the remaining processing steps are similar.

It should also be emphasized that grain boundaries may provide also a positive influence on total oxygen

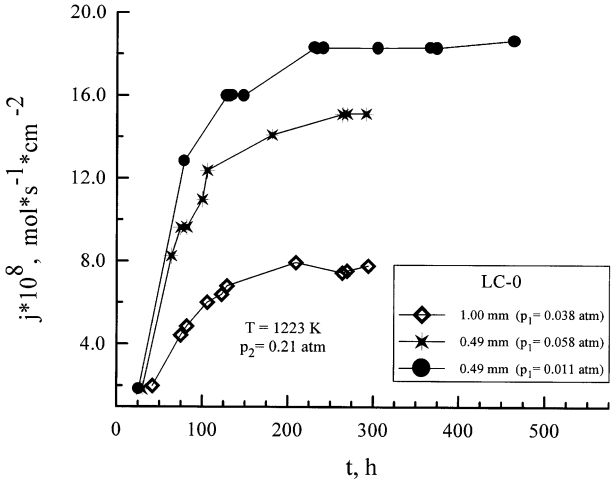

Fig. 7. Time dependence of oxygen permeation fluxes through LC-0 membranes under fixed oxygen partial pressure gradient.

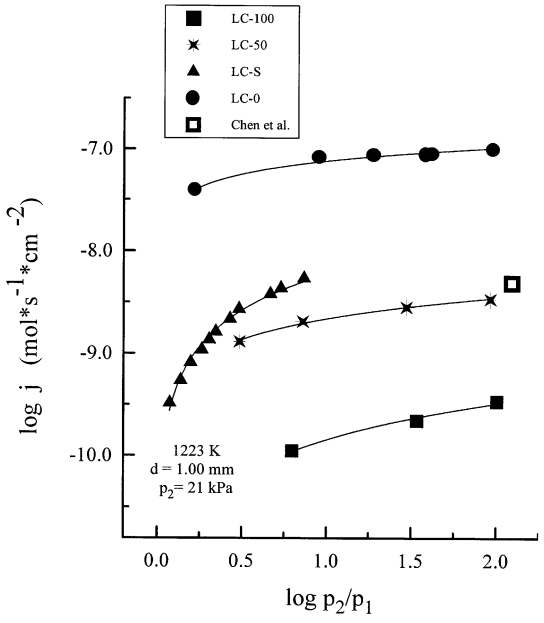

Fig. 8. Dependence of oxygen permeation fluxes through $LaCoO_{3-\delta}$ membranes on oxygen partial pressure gradient at 1223 K. The thickness of all membranes was 1.00 mm, except for LC-S. The fluxes through LC-S ceramics were measured with a 0.90 mm thick membrane and then normalized to 1 mm.

ionic conductivity. When the grain boundary resistance to ionic transport is low enough, an additional contribution to the oxygen transport due to diffusion along grain boundaries may take place. Such behavior is often observed in mixed conductors. As an example, the tracer diffusion coefficients in ceramic grain boundaries of $La_{0.6}Sr_{0.4}Fe_{0.8}Co_{0.2}O_{3-\delta}$ at 660–780 K are higher than the grain bulk diffusion coefficients by a factor of 10^2–10^4.[34] The grain-boundary oxygen diffusion coefficient in A-site-deficient $LaMnO_3$ at 1170 K is three orders of magnitude larger than for the bulk.[35] The already mentioned crystallization of secondary phases along the grain boundaries in LC-0, from amorphous layers formed during a liquid-phase assisted sintering process, may thus justify the high oxygen permeability of LC-0 membranes. This assumption is also in good agreement with the slow increase in the permeation fluxes with time (Fig. 7).

4. Conclusions

Dense $LaCoO_{3-\delta}$ ceramics with different microstructures were prepared using the standard ceramic synthesis route (Method 1), the cellulose-precursor technique (Method 2) and a commercial powder obtained via combustion synthesis. The powders with submicron particle size, formed in Method 2 and via combustion synthesis, exhibit much higher reactivity and sinterability but worse compactability with respect to the powder obtained by the standard ceramic technique. As a large shrinkage may complicate the fabrication of long ceramic parts, a combination of types of powders might be desirable in practical applications such as ceramic membrane production.

The role of processing route on crystal lattice, electronic conductivity and thermal expansion of the materials was found negligible. In contrast, the preparation technique significantly affects the ceramic microstructure and the oxygen ionic conduction. Lanthanum cobaltite membranes prepared by the standard ceramic technique show significantly higher oxygen permeation fluxes than those prepared using organic precursors. This is believed to be caused by a low grain-boundary resistance to oxygen ionic transport. Long stabilization processes under oxygen chemical potential gradients observed for the ceramics prepared by Method 1 may also be explained in terms of the grain-boundary effect.

The obtained results clearly show the importance of microstructural optimization of mixed-conducting ceramic materials for high-temperature electrochemical applications. If the applicability is determined by global electronic transport properties (e.g., current collectors), the synthesis route plays a secondary role and should be selected to provide other necessary parameters such as mechanical strength. However, when the ionic conductivity is important (SOFC electrodes, oxygen membranes), the processing technology should be optimized in order to reduce the grain boundary resistance to oxygen transport.

Acknowledgements

This research was partially supported by and the Belarus Foundation for Basic Research and the FCT (Praxis, Portugal). The authors are sincerely grateful to L.S. Boginsky, A.A. Tonoyan and L.V. Solov'eva for experimental assistance and helpful discussions.

References

1. Anderson, H. U., Review of p-type doped perovskite materials for SOFC and other applications. *Solid State Ionics*, 1992, **52**, 33–41.
2. Mizusaki, J., Nonstoichiometry, diffusion, and electrical properties of perovskite-type oxide electrode materials. *Solid State Ionics*, 1992, **52**, 79–91.
3. Carter, S., Selcuk, A., Chater, R. J., Kajda, J., Kilner, J. A. and Steele, B. C. H., Oxygen transport in selected nonstoichiometric perovskite-structure oxides. *Solid State Ionics*, 1992, **53-56**, 597–605.
4. Bouwmeester, H. J. M. and Burgraaf, A. J., Dense ceramic membranes for oxygen separation. In *Fundamentals of Inorganic Membrane Science and Technology*, ed. A. J. Burgraaf and L. Cot. Elsevier, Amsterdam, 1996, pp. 435–528.
5. De Souza, R. A. and Kilner, J. A., Oxygen transport in $La_{1-x}Sr_xMn_{1-y}Co_yO_{3\pm\delta}$. Part I. Oxygen tracer diffusion. *Solid State Ionics*, 1998, **106**, 175–187.
6. Kharton, V. V., Yaremchenko, A. A. and Naumovich, E. N., Research on the electrochemistry of oxygen ion conductors in the former Soviet Union. II. Perovskite-related oxides. *J. Solid State Electrochem.*, 1999, **3**, 303–326 .
7. Islam, M. S., Ionic transport in ABO_3 perovskite oxides: a computer modelling tour. *J. Mater. Chem.*, 2000, **10**, 1027–1038.
8. Petrov, A. N., Kononchuk, O. F., Andreev, A. V., Cherepanov, V. A. and Kofstad, P., Crystal structure, electrical and magnetic properties of $La_{1-x}Sr_xCoO_{3-y}$. *Solid State Ionics*, 1995, **80**, 189–199.
9. Mizusaki, J., Mima, Y., Yamauchi, S., Fueki, K. and Tagawa, H., Nonstoichiometry of the perovskite-type oxides $La_{1-x}Sr_xCoO_{3-\delta}$. *J. Solid State Chem.*, 1989, **80**, 102–111.
10. Mineshige, A., Kobune, M., Fujii, S., Ogumi, Z., Inaba, M., Yao, T. and Kikuchi, K., Metal-insulator transition and crystal structure of $La_{1-x}Sr_xCoO_3$ as functions of Sr-content, temperature and oxygen partial pressure. *J. Solid State Chem.*, 1999, **142**, 374–381.
11. Senaris-Rodriguez, M. A. and Goodenough, J. B., $LaCoO_3$ Revisited. *J. Solid State Chem.*, 1995, **116**, 224–231.
12. Kharton, V. V., Naumovich, E. N., Vecher, A. A. and Nikolaev, A. V., Oxide ionic conduction in $Ln(Sr)CoO_3$ (Ln = La,Pr,Nd). *J. Solid State Chem.*, 1995, **120**, 128–136.
13. Chen, C. H., Kruidhof, H., Bouwmeester, H. J. M. and Burgraaf, A. J., Ionic conductivity of perovskite $LaCoO_3$ measured by oxygen permeation technique. *J. Appl. Electrochem.*, 1997, **27**, 71–75.
14. Ishigaki, T., Yamauchi, S., Mizusaki, J., Fueki, K. and Tamura, H., Tracer diffusion coefficient of oxide ions in $LaCoO_3$ single crystal. *J. Solid State Chem.*, 1984, **54**, 100–107.
15. Ishigaki, T., Yamauchi, S., Kishio, K., Mizusaki, J. and Fueki,

F., Diffusion of oxide ion vacancies in perovskite-type oxides. *J. Solid State Chem.*, 1988, **73**, 179–187.
16. Figueiredo, F. M., Marques, F. M. B. and Frade, J. R., Electrochemical permeability of $La_{1-x}Sr_xCoO_{3-\delta}$ materials. *Solid State Ionics*, 1998, **111**, 273–281.
17. Kharton, V. V., Naumovich, E. N., Zhuk, P. P., Demin, A. K. and Nikolaev, A. V., Physicochemical and electrochemical properties of $Ln(Sr)CoO_3$ electrode materials. *Russ. J. Electrochem.*, 1992, **28**, 1376–1384.
18. Kharton, V. V., Naumovich, E. N. and Nikolaev, A. V., Materials of high temperature oxygen electrochemical membranes. *J. Membrane Sci.*, 1996, **111**, 149–157.
19. Kharton, V. V., Viskup, A. P., Naumovich, E. N. and Lapchuk, N. M., Mixed electronic and ionic conductivity of $LaCo(M)O_3$ (M = Ga, Cr, Fe or Ni). I. Oxygen transport in perovskites $LaCoO_3$-$LaGaO_3$. *Solid State Ionics*, 1997, **104**, 67–78.
20. Kovalevsky, A. V., Kharton, V. V., Tikhonovich, V. N., Naumovich, E. N., Tonoyan, A. A., Reut, O. P. and Boginsky, L. S., Oxygen permeation through $Sr(Ln)CoO_{3-\delta}$ (Ln = La, Nd, Sm, Gd) ceramic membranes. *Mater. Sci. Eng. B*, 1998, **52**, 105–116.
21. Kharton, V. V., Naumovich, E. N., Kovalevsky, A. V., Viskup, A. P., Figueiredo, F. M., Bashmakov, I. A. and Marques, F. M. B., Mixed electronic and ionic conductivity of $LaCo(M)O_3$ (M = Ga, Cr, Fe or Ni). IV. Effect of preparation method on oxygen transport in $LaCoO_{3-\delta}$. *Solid State Ionics*, 2000, **138**, 135–148.
22. Badval, S. P. S., Zirconia-based solid electrolytes: microstructure, stability and ionic conductivity. *Solid State Ionics*, 1992, **52**, 23–32.
23. Steil, M. C., Thevenot, F. and Kleitz, M., Densification of yttria-stabilized zirconia. Impedance spectroscopy analysis. *J. Electrochem. Soc.*, 1997, **144**, 390–398.
24. Christie, G. M. and van Berkel, F. P. F., Microstructure-ionic conductivity relationships in ceria-gadolinia electrolytes. *Solid State Ionics*, 1996, **83**, 17–27.
25. Kharton, V. V., Naumovich, E. N. and Vecher, A. a., Research on the electrochemistry of oxygen ion conductors in the former Soviet Union. I. ZrO_2-based ceramic materials. *J. Solid State Electrochem.*, 1999, **3**, 61–81.
26. Zhang, K., Yang, Y. L., Ponnusamy, D., Jacobson, A. J. and Salama, K., Effect of microstructure on oxygen permeation in $SrCo_{0.8}Fe_{0.2}O_{3-\delta}$. *J. Mater. Sci.*, 1999, **34**, 1367–1372.
27. Kharton, V. V., Tikhonovich, V. N., Shuangbao, Li, Naumovich, E. N., Kovalevsky, A. V., Viskup, A. P., Bashmakov, I. A. and Yaremchenko, A. A., Ceramic microstructure and oxygen permeability of $SrCo(Fe,M)O_{3-\delta}$ (M = Cu or Cr) perovskite membranes. *J. Electrochem. Soc.*, 1998, **145**, 1363–1374.
28. Solov'eva, L. V., Grigor'eva, I. M., Tikhonova, T. F., Bashmakov, I. A. and Kaputsky, F. N., Structure-modified salt-containing cellulose in metal oxide synthesis. *Vesti AN Belarusi, ser. khim.*, 1994, No 3, 57–61 (in Russian).
29. Kharton, V. V., Naumovich, E. N., Tikhonovich, V. N., Bashmakov, I. A., Boginsky, L. S. and Kovalevsky, A. V., Testing tubular solid oxide fuel cells in nonsteady-state conditions. *J. Power Sources*, 1999, **77**, 242–249.
30. German, R. M., *Sintering theory and practice*. Wiley-Interscience, NY-Chichester-Brisbane-Toronto-Singapore, 1996.
31. van Roosmalen, J. A. M., Huijsmans, J. P. P. and Plomp, L., Electrical conductivity in $La_{1-x}Sr_xMnO_{3+\delta}$. *Solid State Ionics*, 1993, **66**, 279–284.
32. Kharton, V. V., Kovalevsky, A. V., Tikhonovich, V. N., Naumovich, E. N. and Viskup, A. P., Mixed electronic and ionic conductivity of $LaCo(M)O_3$ (M = Ga, Cr, Fe or Ni). II. Oxygen permeation through Cr- and Ni-substituted $LaCoO_3$. *Solid State Ionics*, 1998, **110**, 53–60.
33. ten Elshof, J. E., Bouwmeester, H. J. M. and Verveij, H., Oxygen transport through $La_{1-x}Sr_xFeO_{3-\delta}$ membranes. I. Permeation in air/He gradients. *Solid State Ionics*, 1995, **81**, 97–109.
34. Benson, S. J., Chater, R. J. and Kilner, J. A., Oxygen diffusion and surface exchange in the mixed conducting perovskite $La_{0.6}Sr_{0.4}Fe_{0.8}Co_{0.2}O_{3-\delta}$. In *Ionic and Mixed Conducting Ceramics III*, ed. T. E. Ramanarayanan. The Electrochemical Society, Pennington, NJ, 1998, pp. 596–609.
35. Berenov, A. V., MacManus-Driscoll, J. L. and Kilner, J. A., Oxygen tracer diffusion in undoped lanthanum manganites. *Solid State Ionics*, 1999, **122**, 41–49.